Research Report

Submitted to:

The Oklahoma Water Resource Research Institute

Title:

Estimating the orientation and intensity of fractures in sedimentary rocks using multi-component 3-D ground-penetrating radar (GPR)

Submitted by:

Surinder Sahai, Associate Professor and Geophysics Chair
Oklahoma State University
Roger A. Young, Associate Professor
University of Oklahoma
Todd Halihan, Assistant Professor
Oklahoma State University

Starting Date: 3/1/05

End Date: 2/28/06

Problem and Research Objectives

Fractures in sedimentary rocks influence the hydraulic properties of aquifers. Not only are the fractures important for the flow of water through an aquifer but the recharge of the aquifer is greatly influenced by the fracture aperture, orientation, and density. Therefore, an understanding of the orientation and hydraulic parameters of fractures is crucial to ground water flow modelers in research institutions, and government agencies charged with managing the water resources for the state of Oklahoma (Sahai and others, 2005).

Ground Penetrating Radar (GPR) has been shown to have the potential to detect vertical fractures in sedimentary formations (Tsoflias and others, 2004). Figure 1 illustrates the multicomponent GPR method described by Tsoflias and others (2004). The presence of a fracture affects the phase of the GPR signal differently in the H-polarization and E-polarization. In H-polarization, the magnetic field is parallel to the fracture. In E-polarization, the electric field is parallel to the fracture. By acquiring radar data with different antenna orientations at various angles to the fracture, the phase differences in the receiver signal can be used to determine the presence and orientation of the fracture. Therefore, fracture detection should be possible from polarization studies.

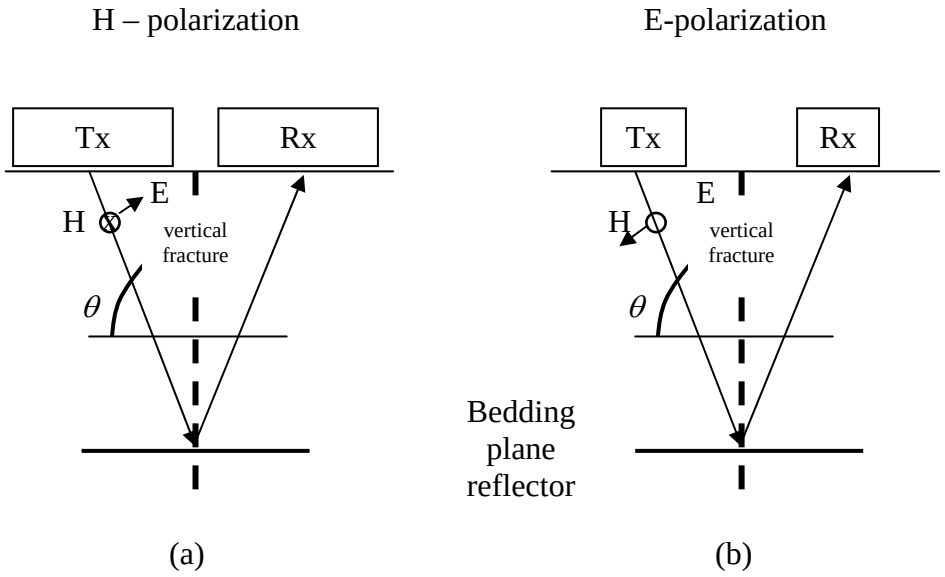

Figure 1. Schematic of the H-polarization and E-polarization response to a fracture at a large angle of incidence. (a) Antennas in endfire orientation. The magnetic field is parallel to the fracture in H-polarization. (b) Antennas in parallel orientation. The electric field is parallel to the fracture in E-polarization. Tx and Rx are the transmitter and receiver antennas respectively and the sizes of the boxes signify the length and width of the antennas. (after Tsoflias et al., 2004).

Tsoflias and others (2001) show that for a horizontal fracture plane, the amplitude of the GPR signal is affected by the fracture aperture and saturation. Therefore, GPR has the potential to not only detect fractures but also provide quantitative information about the hydraulic properties of fractures.

The research work presented in this report was undertaken with the objective of detecting the orientation and intensity of fractures in sedimentary rocks and possibly extend the work of Tsoflias and others (2004). The site selected for our study was a former gypsum quarry in a karstic region of western Oklahoma (Figure 2). The quarry floor is replete with fractures of varying sizes. The dominant fracture trend is NE-SW although there are cross-cutting fractures, as well as some fractures that run predominantly E-W. Many fractures have sub-millimeter apertures while others can be classified as the surface expressions of large sinkholes in the subsurface (Figure 3). In addition to being an ideal place for the investigation of geophysical and hydrological techniques to map fractures in gypsum, the site is also of interest to the Oklahoma Department of Transportation because the karst topography in the area is a potential hazard to the integrity of highways. The geophysical techniques used in our study included Ground Penetrating Radar (GPR) and a Global Positioning System (GPS).

Figure 2. A view of the quarry floor looking east. The fractures in the quarry floor are visible in the foreground.

Figure 3. Some fractures are surface expressions of large sinkholes in gypsum. Buckets of water poured into these fractures disappears quickly.

Methodology

The field work for this project involved GPS mapping, subsurface imaging with ground penetrating radar, and hydraulic testing. The locations of all geophysical observations, geologic mapping, and hydrologic testing were established by differential GPS measurements. A Trimble GPS and base station, Pathfinder software to log waypoints, and ArcView software were used to map important features with a spatial accuracy of 0.1 m. Figure 4 shows the trend of some of the fractures mapped at the survey site, the locations of GPR lines, and polarization and hydraulic tests.

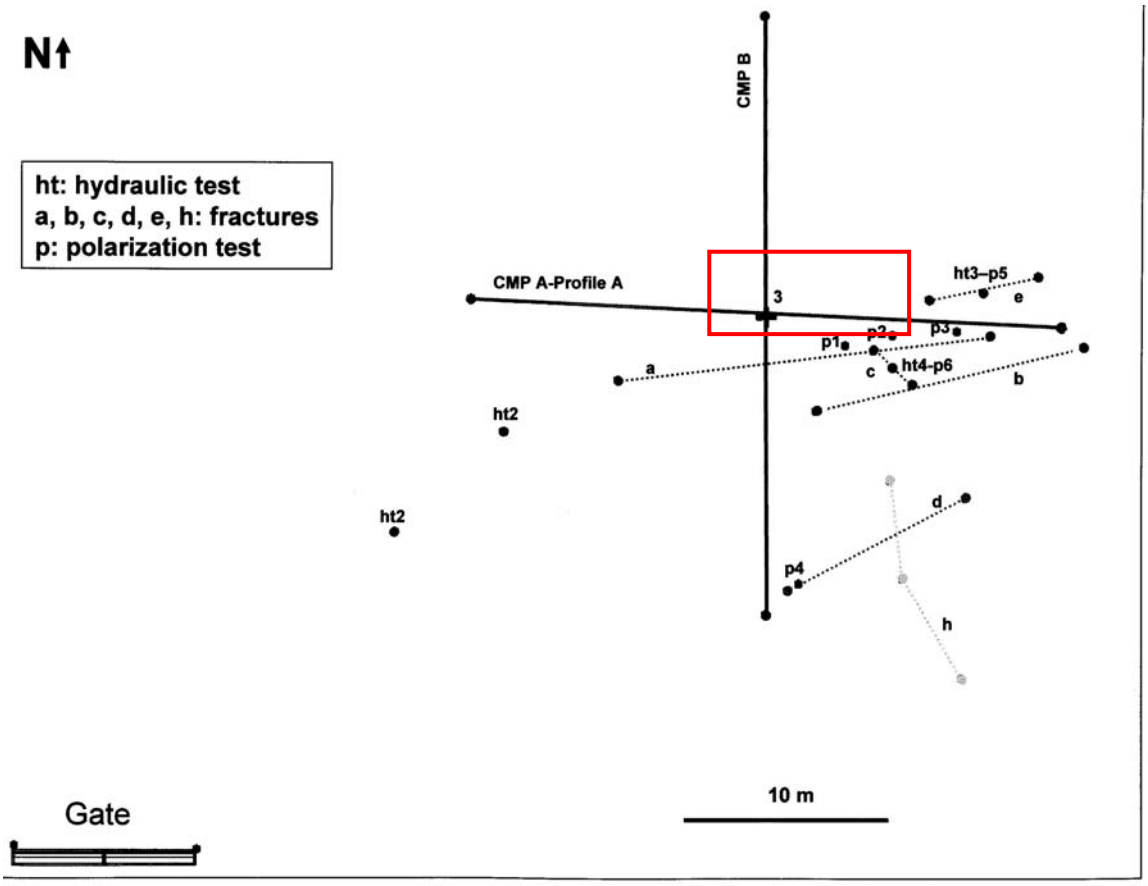

Figure 4. GPS mapped location of some fractures on the quarry floor (dotted lines), the locations of GPR profiles A and B, the locations of common mid-point measurements for radar velocity analyses, and polarization and hydraulic tests. The rectangular box shows the location of 24 common mid-point surveys conducted for mapping the velocity field in the vicinity of the large fracture shown in Figure 3.

The fracture aperture influences the GPR signal polarization. The fracture aperture can be measured directly by mechanical means, i.e., measuring the fracture opening with a fine scaled ruler. This method works well when the fracture aperture is large enough to be measured accurately. Another method is to do infiltration experiments to determine the rate of flow of water through the fracture for a given hydraulic head and then use Darcy's equation to calculate the fracture aperture. In our work, infiltration experiments were conducted by bonding a 6" diameter PVC coupler to the quarry floor using Bondo® body filler (Figure 5). The coupler was filled with water and allowed to infiltrate. The water level change as a function of time was measured with a ruler. In one case, it was difficult to bond the plastic pipe to the quarry floor to produce a water tight seal. In another case, the hydraulic aperture of the fracture was too large to conduct any meaningful measurement of hydraulic conductivity (Figure 3). Therefore, the results for only one fracture (location ht4 in Figure 4) are presented.

Figure 5. Six inch PVC coupler bonded to a NE-SW fracture (left) in preparation for infiltration experiment. The picture on the right shows the polarization experiment Being conducted for dry and saturated fracture conditions.

The GPR data was acquired using standard techniques (Davis and Annan, 1989; Jol and Bristow, 2003). A PulseEkko100 system with 200 MHz antenna was used to image the subsurface with GPR. The antenna spacing of 0.5 m and step size of 0.075 m (3 inches) was used to acquire two N-S and W-E trending GPR lines. These lines were centered on a fracture with a large hydraulic aperture measuring several centimeters (Figure 3). Twenty-four locations were selected for common mid-point data acquisition on a 1m x 1m grid in order to map the velocity field in the vicinity of the fracture seen in Figure 3.

The polarization data was acquired with 100 MHz and 200 MHz transmitter antennas oriented in the parallel and endfire configurations. The experiments with the 100 MHz antenna were conducted in the absence of the infiltration experiments. The 200 MHz data was acquired for both dry and water saturated fracture conditions (Figure 5). Figure 6 shows the antenna configuration used to acquire the polarization data.

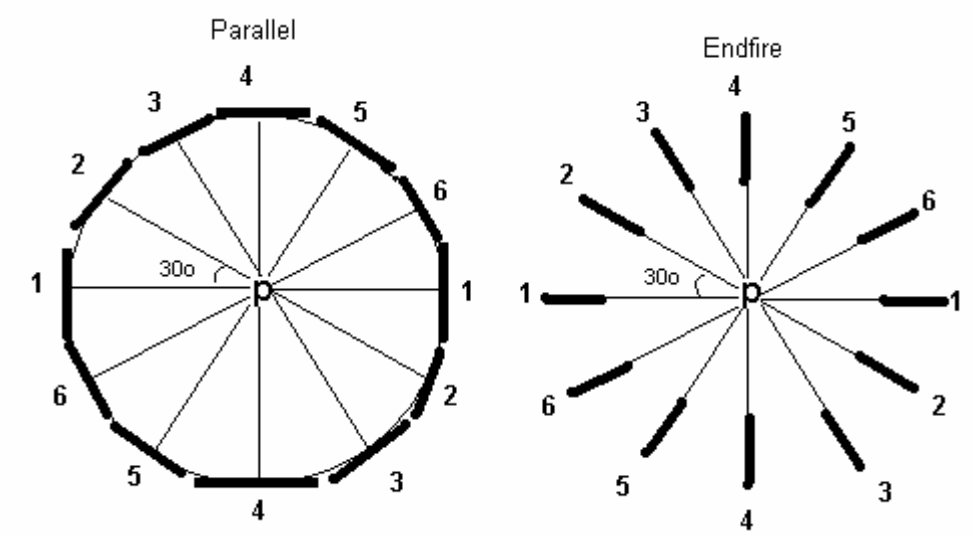

Figure 6. The parallel and endfire antenna configurations. The transmitter-receiver pair was rotated by 30 degree increments to complete a circle around a fracture.

Results and Discussion

Figure 7 shows the water infiltration data obtained from fracture h4 (Figure 4). The fluid flow through the fracture is steady because the rate of change of water level in the PVC coupler is directly related to the elapsed time. Therefore, a straight line relationship can be used to determine the rate of infiltration through the fracture. The fracture aperture "b" can be calculated from the well known Darcy's equation:

$$Q = K I A$$

where Q is the infiltration rate, K is the hydraulic conductivity, I is the hydraulic gradient, and A is the surface area of the fracture. The area is related to the fracture aperture b and width w by:

$$A = b w$$

The width of the fracture in our case is the diameter of the PVC coupler.

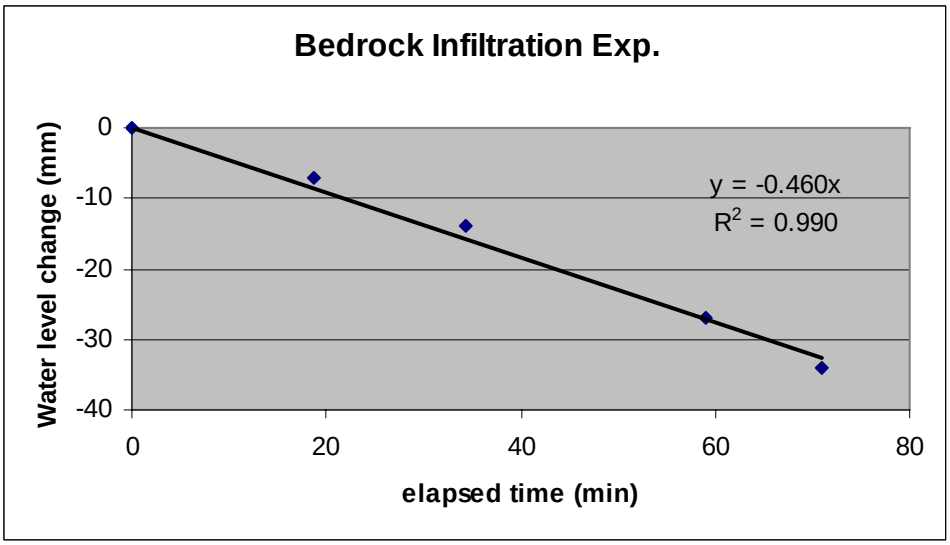

Figure 7. The change in water level in the PVC coupler plotted as a function of elapsed time for fracture h4 (figure 4).

From our data, the bulk infiltration rate for fracture h4 was calculated to be 7.66×10^{-6} m/s. Assuming a hydraulic gradient of 1.0 for the fracture, the hydraulic conductivity of the fracture is 8.49×10^{-3} m/s which corresponds to a hydraulic fracture aperture of 0.108 mm or 108 microns. A large number of fractures visible in the quarry floor seem to have similar apertures. Although an individual fracture of sub-millimeter aperture may have very little influence on the GPR polarization results (Tsoflias, personal communication), a large number of fractures (thus high fracture density) may result in a measurable polarization effect on the GPR signal.

Knowledge of the velocity of radar waves at the gypsum quarry site is important for converting a time section to a depth section. Moreover, the velocity field at the site can aid in the interpretation of the subsurface geology. Figure 8 shows a typical common mid-point gather obtained at the site. The direct waves traveling from the transmitter to the receiver appear as linear events on the time versus offset position plot on the left. The reflection events are hyperbolic in appearance. It is these events that are important for determining the velocity. The right hand side of Figure 8 shows the semblance plot generated from the common mid-point data. The velocity at a point in depth is given by the bull's-eye picks on the semblance plot. Two observations can be made from this plot. First, the velocity of radar waves in gypsum is of the order of 0.1 m/ns. Second, there is a slight increase in velocity with depth. We used a velocity of 0.1 m/ns to convert the time to depth sections.

Figure 9 shows an east-west GPR line (marked A in Figure 4). It is apparent that the data is replete with diffractions that possibly result from sharp discontinuities in the subsurface. Some examples of these discontinuities are faults and fracture, and in our case, possibly sinkholes. The GPR profile shows a lack of horizontal bedding within the gypsum. Instead small relief depocenters and fractures are abundant throughout the section.

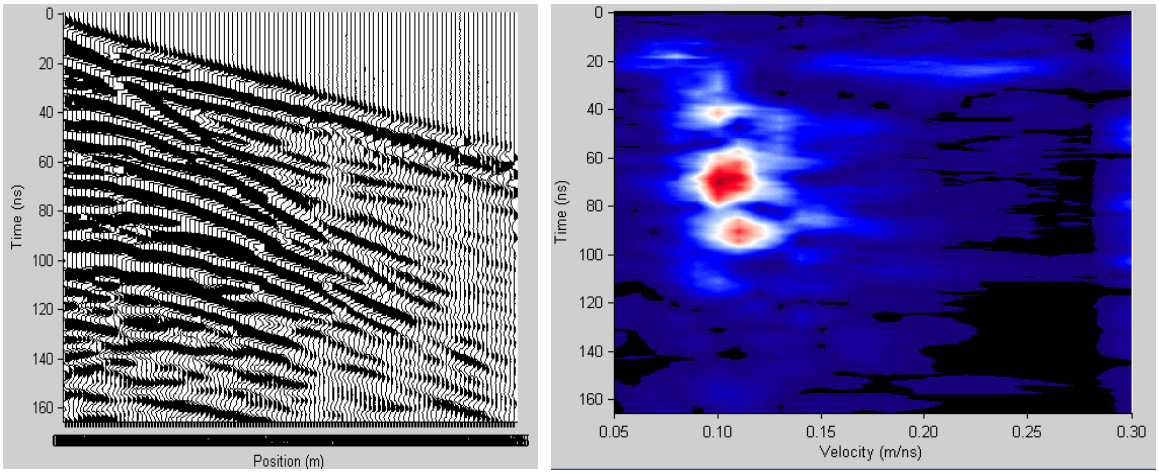

Figure 8. A common mid-point profile (left) and the corresponding semblance plot (right) for velocity picks.

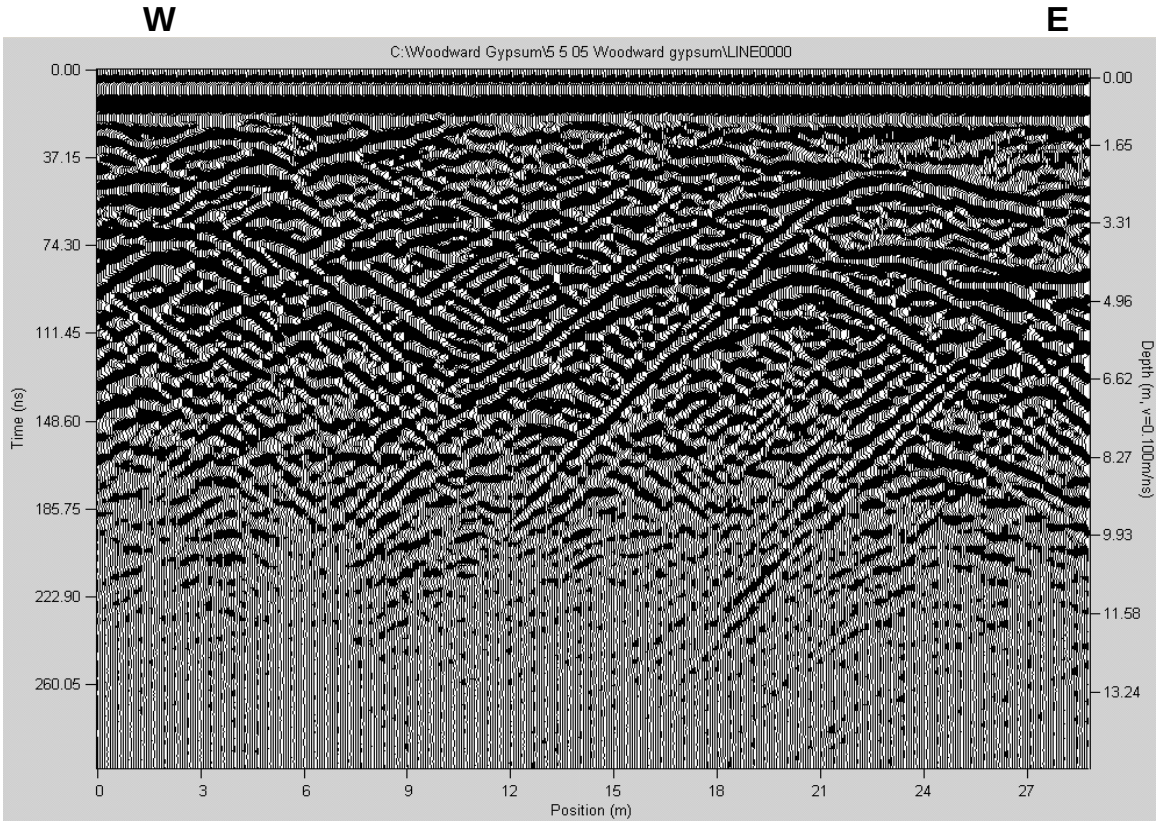

Figure 9. An east-west GPR line (line A in figure 4). The diffractions are the result of faults and fractures, and possibly sinkholes in gypsum. The large fracture shown in Figure 3 is located at the center of the line.

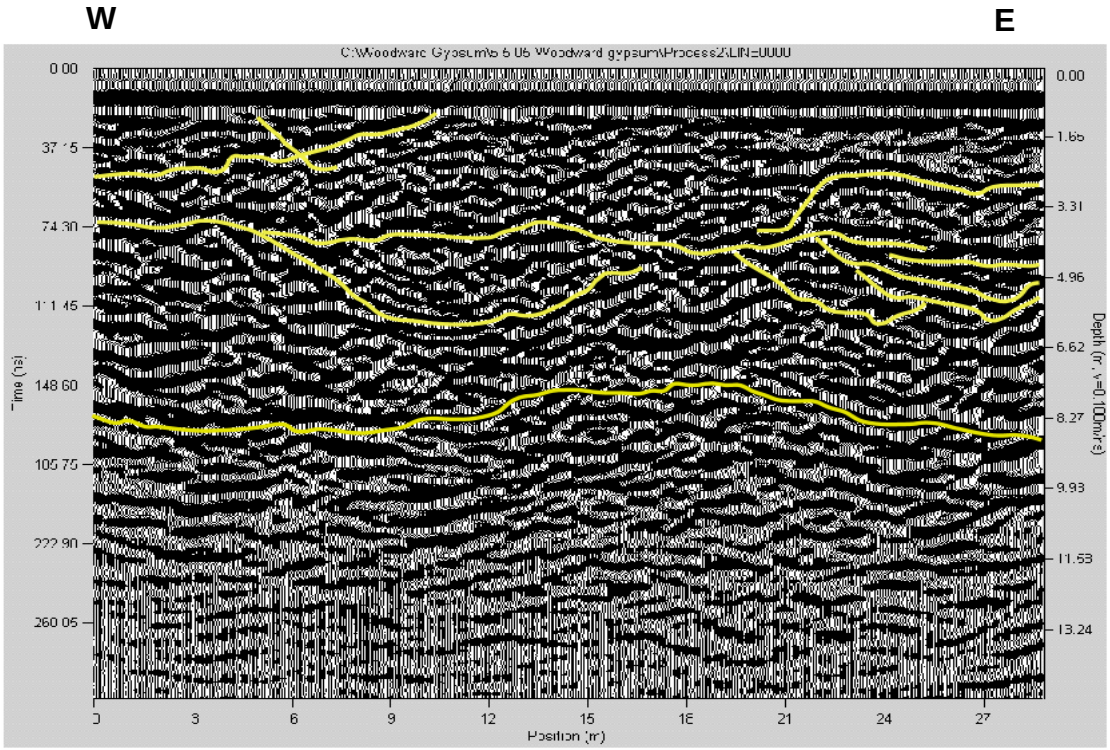

Figure 10. Migration of line A shown in figure 9. The diffraction energy is collapsed, revealing highly irregular subsurface.

Many applications of GPR involve detection of buried objects such as pipelines, rebar, etc. These objects produce diffractions which are used as indicators of their presence or absence. However, diffractions obscure geological information. Migration of GPR data is necessary to collapse the diffraction energy to the point of origin. Figure 10 shows the migrated data for line A. The discontinuous nature of the subsurface is quite evident in this data. There are numerous fractures and faults beneath the quarry floor. A synclinal feature between 75 and 120 nsec (approximately 4 to 6 meter depth) could be a sinkhole or collapsed feature because the large fracture (Figure 3) is at the center of line A. A map of the radar velocity field is shown in Figure 11. A high velocity anomaly is centered in the vicinity of the large fracture which could be further evidence of a sinkhole. As noted previously, the hydraulic conductivity of the large fracture could not be measured. The water disappeared in the fracture as fast it could be poured.

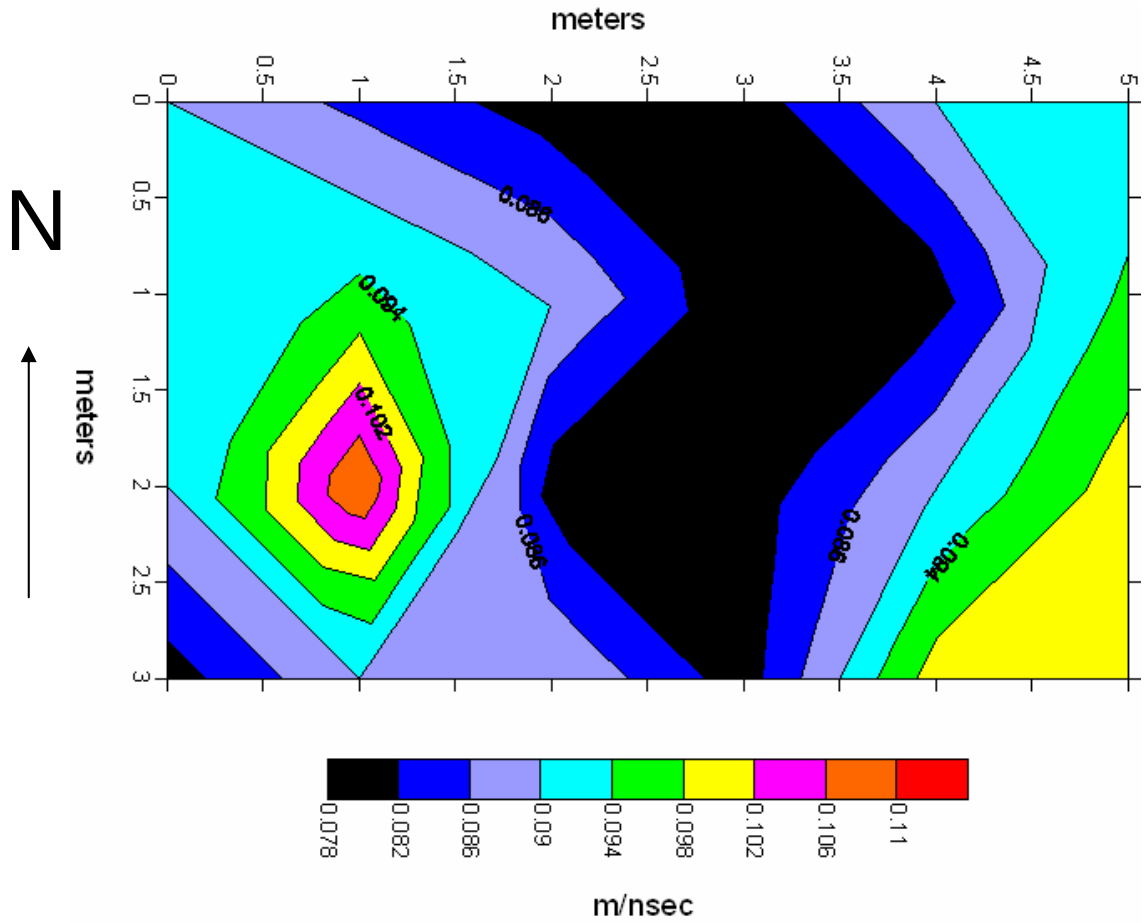

Figure 11. The radar velocity field in the area of the large fracture (figure 3). The high velocity (bull's-eye in the lower left) occurs in the vicinity of the fracture. The velocity variations are predominantly in an east-west direction.

The GPR polarization tests performed across fracture ht4 for both the dry and wet fracture are shown in Figure 12. Five traces in succession were recorded at each location occupied by the transmitter-receiver pair. When the GPR transmitter is fired, the generated E-field of the electromagnetic pulse is parallel to the length of the transmitter antenna. Figures 12 shows that there are definite differences in the arrival time of the GPR signal when the data are acquired in the parallel or endfire configuration, i.e., the E-field is parallel or perpendicular to the fracture. The delay times translate into phase differences between the recorded signals. The data acquired with the endfire configuration appears to have higher frequency content than the parallel configuration data. In the parallel configuration (a and c), there is a slight delay in the reflector time in the shallow section when the electric field is oriented perpendicular to the fracture (orientation c) than parallel to the fracture (orientation a). This is consistent with the work of Tsoflias and others (2004). However, there are large differences in reflector times greater than 60 nsec in panels a and c or b and d that cannot be explained by the presence of a fracture with an aperture of only 0.108 mm. One plausible explanation is

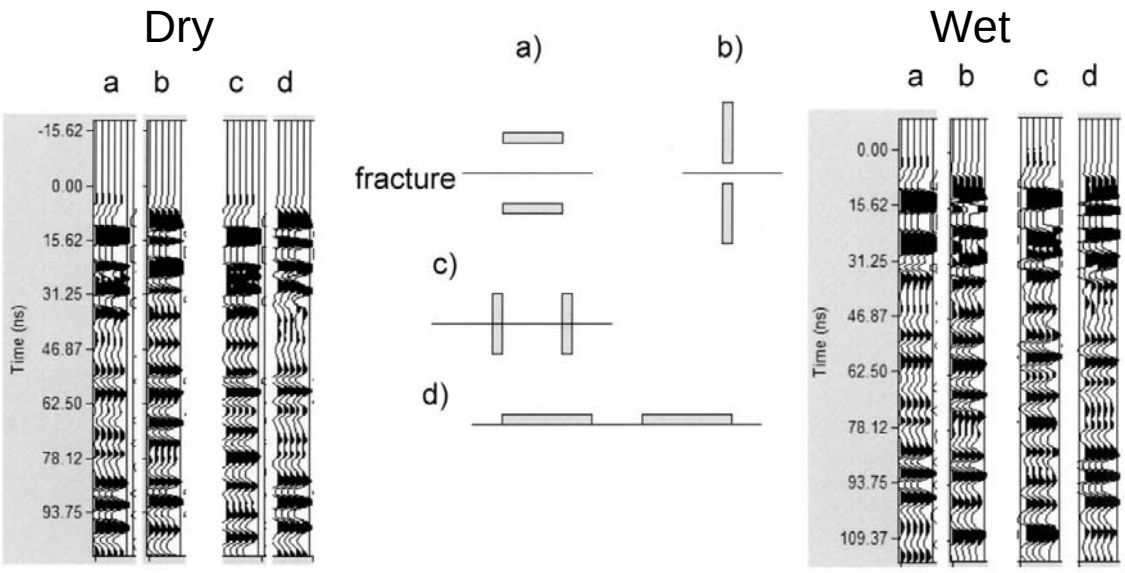

Figure 12. Comparison of parallel and endfire antenna configurations for dry and wet fractures.

the velocity anisotropy due to karst features below the quarry floor (Tsoflias, personal communication).

Figure 13 shows a comparison of the reflection event times for the dry and wet fracture for the endfire antenna configuration. The electric field is perpendicular to the fracture for the zero degree case. The antenna pair was rotated by 30 degree increments around the fracture. In the shallow section, there is a delay in the arrival times of the reflectors when the electric field is perpendicular to the fracture. As the antenna pair is rotated around the fracture, the arrival times get smaller until the electric field is parallel to the fracture. Once again this is consistent with theory. One major difference between the dry and wet case is the highlighted zone where the amplitude and frequency content of the events is greater for the wet fracture than the dry fracture, even though the hydraulic fracture aperture is only 0.108 mm. Therefore, small fracture aperture can lead to measurable change in the amplitude and frequency of the recorded signal. As noted previously, large differences in reflector times below about 60 nsec in various panels are present. Once again, these differences cannot be explained by the presence of a fracture with an aperture of only 0.108 mm.

Another test of the polarization effects on radar waves at fracture h4 (figure 4) was conducted. In this example, the 100 MHz transmitter antenna was used. The antennas were rotated by 45 degrees around the fracture for the parallel and endfire configurations and three traces were acquired at each location. Analyses of reflection delay times were translated into phase differences. Figures 14 and 15 show the cumulative phase for the average trace plotted against time for the four main orientations of the antennas around

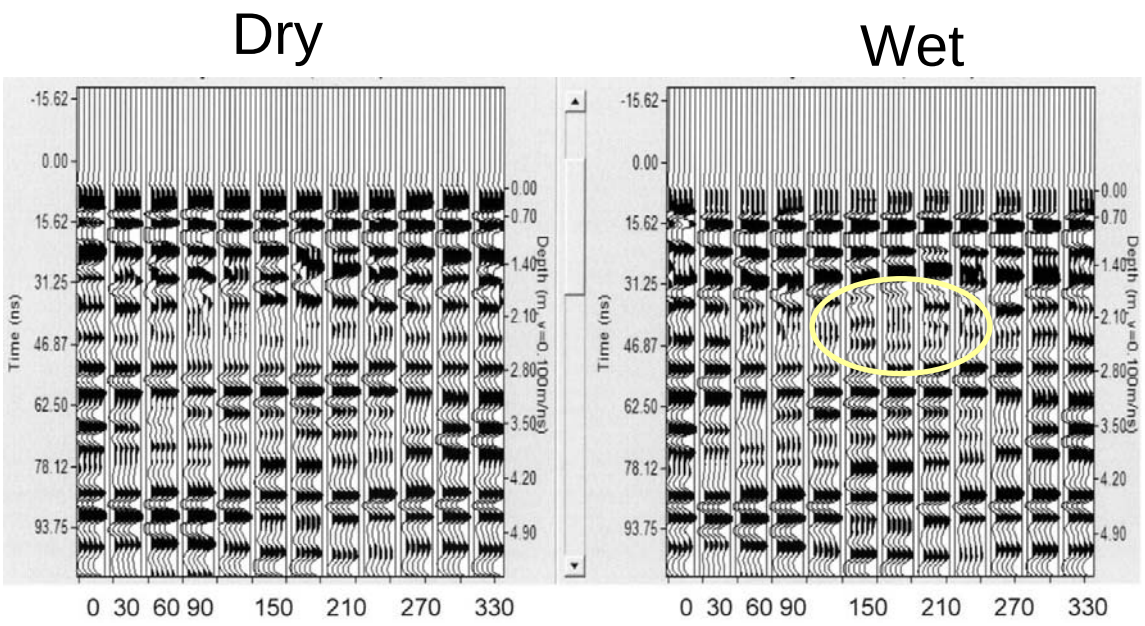

Figure 13. Comparison of dry and wet fracture response at different angles of antenna orientation for the endfire configuration. The electric field is perpendicular to the fracture for the zero degree case.

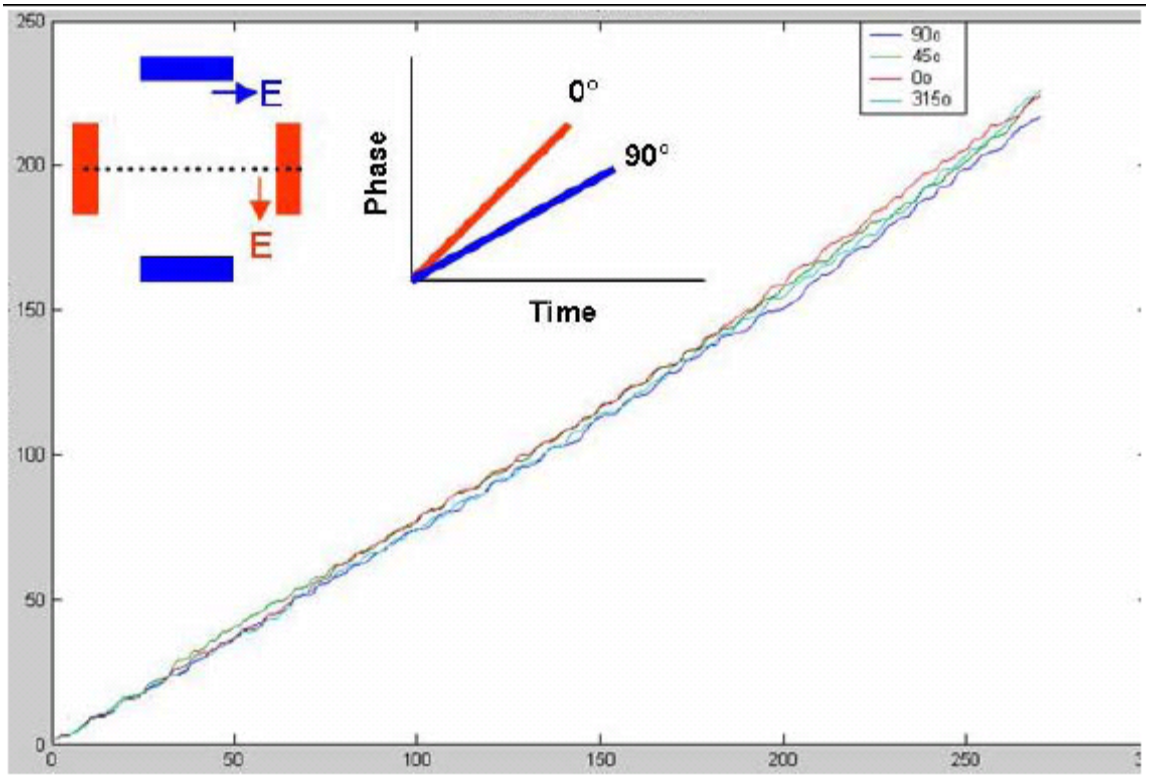

Figure 14. Plot of cumulative phase (vertical axis) and time in nsec (horizontal axis) for the parallel antenna configuration. The inset shows a hypothetical phase plot color-coded to correspond with the colors on the antenna orientations.

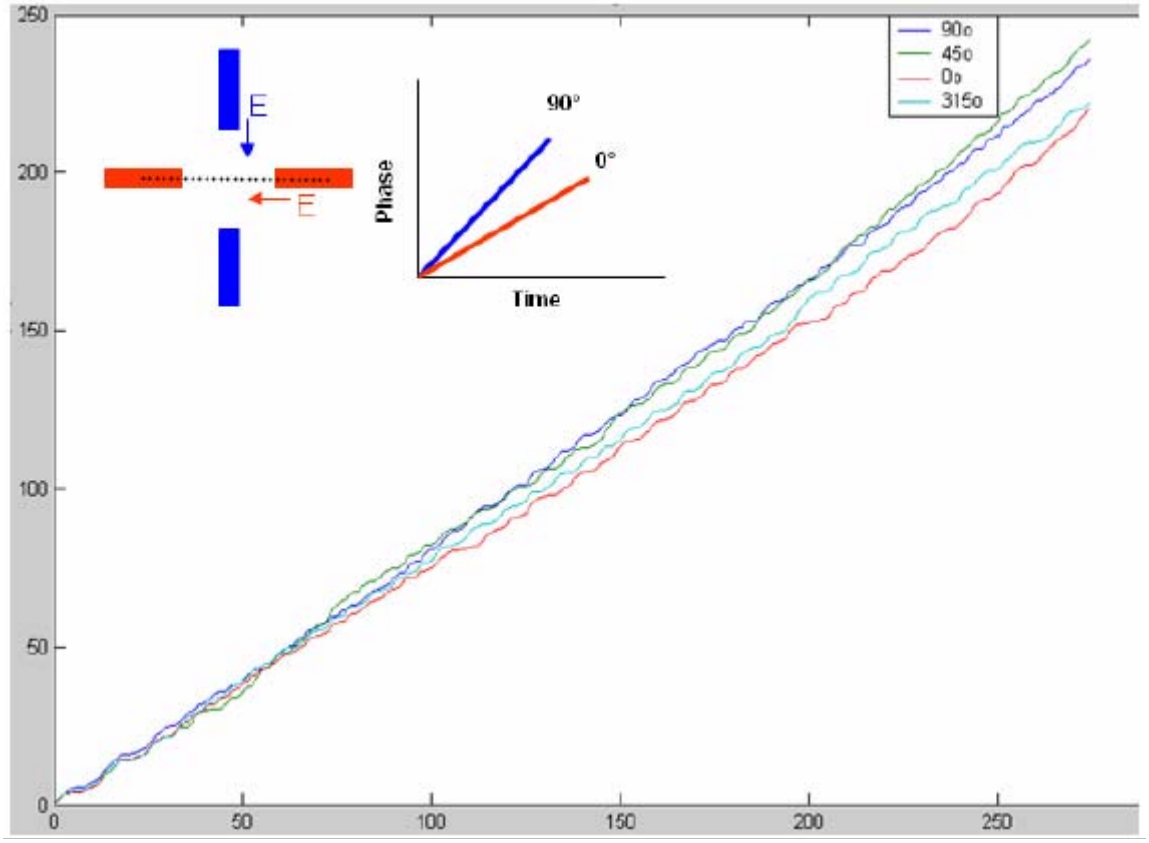

Figure 15. Plot of cumulative phase (vertical axis) and time in nsec (horizontal axis) for the endfire antenna configuration. The inset shows a hypothetical phase plot color-coded to correspond with the colors on the antenna orientations.

the fracture. For the parallel configuration case (Figure 14), the average trace recorded at 0 deg with respect to the fracture plane is expected to experience a greater time delay since the electric field is oriented perpendicular to the fracture plane. A bigger positive phase shift is therefore visible on the plot with respect to the other traces recorded at different orientations. On the other hand, the average trace recorded at 90 degrees with respect to the fracture plane is expected to experience a smaller time delay since the electric field is now oriented parallel to the fracture plane. In this case, the trace is less affected by the presence of the fracture and its cumulative phase response with time is plotted below the other traces. For the endfire case (Figure 15), the resulting phase response is reversed.

Conclusions

The azimuth of fractures can be determined by exploiting the polarization properties of GPR signals because EM waves are affected by the presence of fractures in the subsurface. The orientation of the electric field with respect to the fracture plane affects the reflection time of events on the GPR data. The delay times observed at different antenna orientations and configurations can be quantified into phase information of the recorded traces.

The velocity field at the survey area is laterally heterogeneous. Further careful work on velocities may lead us to a method to predict underground karst features, thus complementing the work reported by other workers (e.g., Tarhule and others, 2003).

The saturated vertical fractures increase the amplitude and frequency of the recorded signal. The increase in amplitude is consistent with the work reported in the literature (Tsoflias and others, 2001). However, the effect on the frequency content of the signal is a new observation and should be confirmed by additional data and analysis.

Bonding a PVC coupler to the quarry floor is an easy and reliable method for determining the fracture aperture. However, further work is needed to understand the relationship between hydraulic conductivity and the attributes of the GPR data.

Recommendations

The gypsum quarry site is probably not an ideal place to conduct GPR multicomponent surveys because the karst features greatly influence the polarization data. At the outset, the gypsum site seemed an ideal place to carry out this work due to easy accessibility and interest by the Oklahoma Department of Transportation (Sahai and others, 2005). Our recommendation is that further studies should be conducted at a different site.

The GPR profiles and common mid-point data should be acquired by using various configurations of the transmitter-receiver antennas. Soon and others (2001) have suggested that fractures with different azimuths can be preferentially imaged depending of on the configuration used when running the GPR profiles.

Acknowledgements

We are grateful to the Oklahoma Water Resources Research Institute (OWWRI) for financial support of this project. Thanks are due Mr. Steve Redgate for permission to access the gypsum site. The students from the OU (David Ramirez-Mejia) and OSU (Chales Kaun and Chris Ennen) assisted with data acquisition and analysis. Thanks are also due Steve Hadaway for help with the field work and Dr. George Tsoflias for consultation on this project.

Publications Cited

Refereed Journals

Davis, J.L. and Annan, A.P., 1989, Ground-penetrating radar for high-resolution mapping of soil and rock stratigraphy: Geophysical Prospecting, 37, 531-551.

Jol, H.M. and Bristow, C.S. 2003, GPR in sediments: advice on data collection, basic processing and interpretation, a good practice guide. In Bristow, C.S. and Jol, H.M. (Editors.): Ground Penetrating Radar in Sediments: Geological Society of London Special Publication 211, p. 9-27.

Soon, J. S., Jung-ho, K., Yoonho, S., Seung-Hwan, C., 2001, Finding the Strike Direction of Fractures using GPR, Geophysical Prospecting, v. 49. p. 300-308.

Tarhule, A., Dewers, T., Young, R.., Witten, A., and Halihan, T., 2003, Integrated subsurface-imaging techniques for detecting cavities in the gypsum karst of Oklahoma, in Johnson, K.S., and Neal, J.T. [eds.], Evaporite karst and engineering/environmental problems in the United States: Oklahoma Geological Survey Circular 109, 77-84.

Tsoflias, G.P., T. Halihan, and J.M. Sharp, Jr., 2001. Monitoring pumping test response in a fractured aquifer using ground-penetrating radar. *Water Resources Research*, v. 37, n. 5, p. 1221-1229.

Tsoflias, G. P., Van Gestel, J. P., Stoffa, P., Blankenship, D. and Sen, M., 2004, Vertical Fracture Detection by Exploiting the Polarization Properties of GPR Signals, Geophysics, v. 69, no. 3, p. 803-810.

Other Publications

Sahai, S., Young, R. A., Halihan, T., 2005, Estimating the orientation and intensity of fractures in sedimentary rocks using multi-component 3-D ground-penetrating radar (GPR), Research Proposal submitted to the Oklahoma Water Resource Research Institute (OWRRI), Project No. AA 587915.